IEEE Access
Multidisciplinary | Rapid Review | Open Access Journal

Received May 6, 2019, accepted May 18, 2019, date of publication May 22, 2019, date of current version June 3, 2019.

Digital Object Identifier 10.1109/ACCESS.2019.2918266

Optical Adaptive Antenna Array for Multiuser Mobile Optical Communication

HAIBO WANG, (Member, IEEE), ZAICHEN ZHANG, (Fellow, IEEE), JIAN DANG, (Member, IEEE), AND LIANG WU, (Member, IEEE)
National Mobile Communications Research Laboratory, Southeast University, Nanjing 210096, China

Corresponding author: Zaichen Zhang (zczhang@seu.edu.cn)

This work was supported by the NSFC under Project 61571105, Project 61871111, Project 61501109, and Project 61601119, and Zhishan Youth Scholar Program Of SEU.

ABSTRACT In this paper, an optical adaptive antenna array system for multi-user optical mobile communication is studied. A coherent signal source is embedded in a spherical optical phased cell array with an external spherical lens system. The system can predict the signal power of the receiving end according to the channel transfer matrix and perform power compensation when transmitting the signal. Correspondingly, a pure phase lossless desired light field recovery algorithm is proposed and used for space division multiple access and free power allocation of antenna array systems. A small-scale optical adaptive antenna array experimental system is built and tested with good performance and consistent with the expected results.

INDEX TERMS Adaptive antenna array, optical mobile communication, phased cell array, space division multiplexing access, free power allocation.

I. INTRODUCTION

With the demand for communication capacity and speed rapidly increasing, the communication band gradually develops higher. Compared with wireless radio frequency (RF) communication, optical wireless communication has high communication capacity, high directivity, strong electromagnetic interference resistance and small size antenna. At the same time, technologies such as beamforming and space division multiple access(SDMA) [1], [2], which have been widely used in fifth-generation(5G) systems, mark the future development of signals in the direction of concentration, directivity and mobility. The characteristics of energy concentration and high directivity of the optical signal itself show special advantages under this development trend. Thus optical SDMA [3], [4] and optical mobile communication (OMC) [5], [6] are valuable research directions that can be realized.

In 5G system, people use the massive multiple input multiple output(MIMO) technology to interfere with the RF signals from different antennas to achieve directional transmission of signals [7], [8]. Although the light itself has strong directivity, in the case of multiple mobile users, it is difficult for the light source to follow multiple targets to adjust the direction, and the adjustability of the signal power distribution is poor. Drawing on the millimeter-wave multi-antenna interference technique, we use optical antenna arrays to intervene in the optical field to obtain accurate optical signal distribution.

Compared with the RF multi-antenna system in 5G technology [9]–[11], the technical concept of this paper has common point. However, the main body of this paper is in the optical frequency band, and techniques such as holographic optics and optical phased arrays are used. At the same time, since the channel modeling of medium-range optical wireless communication does not consider multipath and fading problems [12]–[15], the focus of this paper is on the holographic reconstruction model and hardware experiment of optical signals. Compared with the traditional optical antenna [16]–[19], the optical antenna studied in this paper is oriented to multi-user mobile communication, and a new optical antenna energy distribution scheme is proposed.

Other Sections of this paper is as follows, Section 2 performs channel modeling on OMC, and proposes a power allocation optimization scheme according to the received signal of mobile terminal. Section 3 proposes a structure of optical adaptive antenna array, builds its optical field model, and analyzes the diffraction light field distribution after eliminating the amplitude phase distortion caused by the lens system. Section 4 calculates the desired light field

The associate editor coordinating the review of this manuscript and approving it for publication was Weiren Zhu.

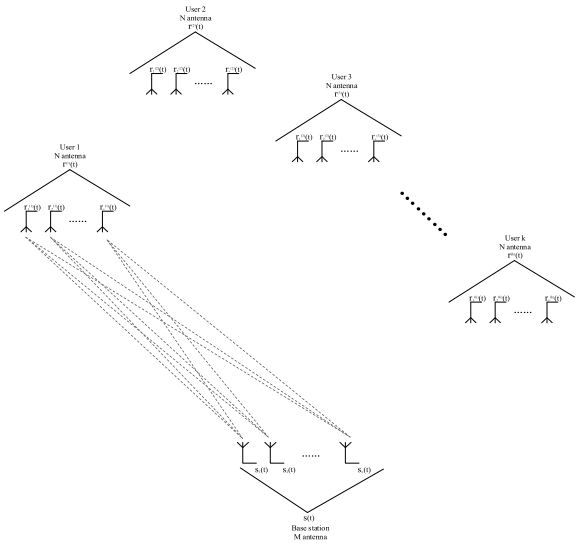

FIGURE 1. MIMO optical mobile communication system.

function according to the power allocation scheme proposed in Section 2, and reproduces the desired light field without loss based on the model in Section 3, achieving space division multiplexing and free power allocation. Section 5 builds a small-scale optical adaptive antenna array for performance testing and evaluation. Section 6 is the experimental result. Conclusions are presented in section 7.

II. OMC CHANNEL MODELING

Fig. 1 is a block diagram of a MIMO OMC system. Assuming that the base station have M antennas, and each mobile user has N receiving antennas, then the base station transmitting signal can be expressed as

$$s(t) = [s_1(t), s_2(t), \ldots, s_M(t)]^T \tag{1}$$

$s_m(t)$ represents the signal of the mth antenna. $[.]^T$ indicates transposition.

Similarly, the received signal of the kth mobile user can be expressed as

$$r^{(k)}(t) = \left[r_1^{(k)}(t), r_2^{(k)}(t), \ldots, r_N^{(k)}(t)\right]^T \tag{2}$$

Because of the nature of light, in the medium-range optical wireless communication scenario, we usually ignore the effects of multipath and fading. So we build a channel transfer matrix H_k

$$H_k = \begin{bmatrix} h_{11}^{(k)} & h_{12}^{(k)} & \cdots & h_{1M}^{(k)} \\ h_{21}^{(k)} & h_{22}^{(k)} & \cdots & h_{2M}^{(k)} \\ \vdots & \vdots & \ddots & \vdots \\ h_{N1}^{(k)} & h_{N2}^{(k)} & \cdots & h_{NM}^{(k)} \end{bmatrix} \tag{3}$$

$h_{nm}^{(k)}$ represents the channel gain of the mth antenna of the base station to the nth antenna of the kth user. Thus, the received

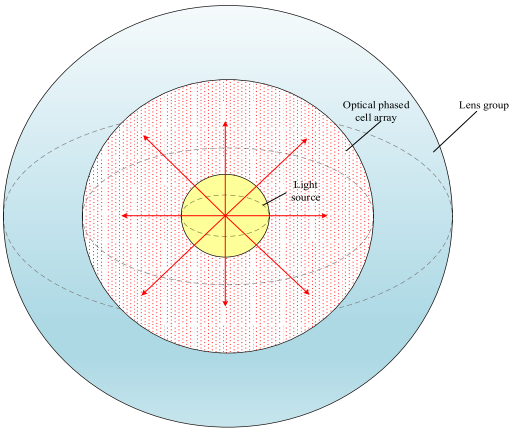

FIGURE 2. Optical adaptive antenna array structure.

signal can be represented as a superposition of the transmitted signal

$$r^{(k)}(t) = \sum_{n=0}^{N} r_n^{(k)}(t) + l(t) = \sum_{n=0}^{N}\sum_{m=0}^{M} s_m(t)h_{nm}^{(k)} + l(t) \tag{4}$$

$l(t)$ represents noise. In order to improve energy efficiency, we can estimate the channel transfer matrix and correct the transmitted signal. Define $s'_m(t)$ as

$$s'_m(t) = \alpha_m^{(k)} s_m(t) \tag{5}$$

where $\alpha_m^{(k)}$ is the correction factor.

$$\alpha_m^{(k)} = \frac{N}{\sum_{n=0}^{N} h_{nm}^{(k)}} \tag{6}$$

Corrected received signal of the kth user

$$r^{(k)'}(t) = \sum_{n=0}^{N}\sum_{m=0}^{M} s'_m(t)h_{nm}^{(k)} + l(t) \tag{7}$$

The optical adaptive antenna array needs to adjust the holographic light field parameters according to the predicted user received signal $r^{(k)'}(t)$ for power distribution. This will be discussed in the following sections.

III. ARRAY STRUCTURE AND LIGHT FIELD MODELING

A. ANTENNA ARRAY STRUCTURE

Fig. 2 is a structure of an optical adaptive antenna array. We use a combination of a single point source, an optical phased cell array, and a lens group system to implement the functionality of a conventional adaptive antenna set. The light source plus an optical phased cell can be regarded as a transmitting antenna that emits parallel light of different phases. The advantages of this structure are that a single light source ensures that all outgoing light is coherent, and the system complexity is low, which transforms the interference problem of multiple phase sources into the phase modulation problem of the phased cell array. Fig. 3 is a regional developed pattern of the optical phased cell array. Each rectangular pixel represents an optical phased cell that freely adjusts the phase of the incident light. The phase-modulated outgoing

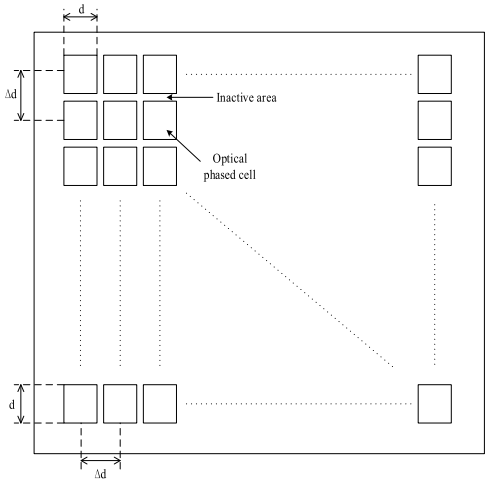

FIGURE 3. Regional developed pattern of the optical phased cell array.

light is concentrated by the lens system, the in-phase light is enhanced, and the anti-phase light is attenuated, thereby achieving focusing of the light beam at a specific position.

B. OPTICAL FIELD MODEL OF ANTENNA ARRAY

In Fig.3, when the number of optical phased cells is infinite, the spacing between cells can be considered as zero. However, under non-ideal conditions, there exists a gap between phased cells and area without phase modulation at the edge of the cell. Therefore, we call the cell gap inactive area when modeling, indicating a region without phase modulation. Assuming that the number of phased cells per unit area is $M' \times N'$, the side length of the phased cell is d, the cell spacing is Δd. The light transmittance function of this phased cell array is

$$t(x,y) = a(x,y)\{\, rect(\frac{x}{d},\frac{y}{d}) \otimes q(x,y) + [\, rect(\frac{x}{\Delta d},\frac{y}{\Delta d}) - rect(\frac{x}{d},\frac{y}{d})\,] \otimes p(x,y)\,\} \quad (8)$$

(8) shows the amplitude distribution of Gaussian light passing through the array, where $\otimes$ represents the convolution operation and $rect(.)$ is a rectangular function, $a(x,y)$, $q(x,y)$, $p(x,y)$ in (1) are as follows:

$$a(x,y) = rect\left(\frac{x}{M'\Delta d},\frac{y}{N'\Delta d}\right) = rect\left(\frac{x}{M'\Delta d}\right) rect\left(\frac{y}{N'\Delta d}\right) \quad (9)$$

$$q(x,y) = e^{i\varphi} \sum_{m=0}^{M'-1}\sum_{n=0}^{N'-1} \delta(x - m\Delta d, y - n\Delta d) \quad (10)$$

$$p(x,y) = e^{i\varphi_c} \sum_{m=0}^{M'-1}\sum_{n=0}^{N'-1} \delta(x - m\Delta d, y - n\Delta d) \quad (11)$$

φ is the phase distribution of optical phased cells. φ_c is the phase shift of the inactive area, which is a constant. In Fig. 3, due to the inactive area, $\Delta d > d$, so $[\, rect(\frac{x}{\Delta d},\frac{y}{\Delta d}) - rect(\frac{x}{d},\frac{y}{d})\,] \otimes p(x,y) < 0$. That causes the loss of optical power, proportional to (Δd-d).

C. DIFFRACTION LIGHT FIELD RECONSTRUCTION AFTER SUPERPOSITION OF FOURIER LIGHT FIELD

Light emitted from an array of optical phase elements needs to pass through a lens system for interference. The process that light passing through the lens is a Fourier transform [20], [21], and the amplitude and phase of signal are distorted. Therefore, at the optical phased cell array we need to superimpose a Fourier light field to cancel the signal distortion caused by the lens group. The reconstructed light field distribution function $T(u,v)$ is the Fourier transform of the original transmittance function $t(x,y)$

$$T(u,v) = A(u,v) \otimes \Big\{ d^2 sinc(ud, vd) Q(u,v) + \Big[\Delta d^2 sinc(u\Delta d, v\Delta d) - d^2 sinc(ud, vd)\Big] P(u,v)\Big\} \quad (12)$$

where

$$A(u,v) = F\{\, a(x,y)\,\} \quad (13)$$

$$Q(u,v) = F\{\, e^{i\varphi}\,\} \otimes \sum_{m,n=-\infty}^{\infty} \delta\left(u - \frac{m}{\Delta d}, v - \frac{n}{\Delta d}\right) \quad (14)$$

$$P(u,v) = F\{\, e^{i\varphi_c}\,\} \otimes \sum_{m,n=-\infty}^{\infty} \delta\left(u - \frac{m}{\Delta d}, v - \frac{n}{\Delta d}\right) \quad (15)$$

when $u = v = 0$

$$T(0,0) = d^2 Q(0,0) + (\Delta d^2 - d^2) P(0,0) = [\mu Q(0,0) + (1-\mu) P(0,0)]/\Delta d^2 \quad (16)$$

The first term $d^2 Q(0,0)$ is the desired light field superimposed on the Fourier light field, and the second term $(\Delta d^2 - d^2)P(0,0)$ is a zero-order diffraction component, which is caused by the inactive area of optical phased cells. Since $P(0,0)$ is a constant value, the second term is equivalent to a beam of in-phase parallel light. Therefore, after recovery by the lens, the zero-order diffraction image is a spot whose intensity is inactive with phased cells. We can occlude it or use this part of the light to locate the beam coverage area.

IV. OPTICAL SPACE DIVISION MULTIPLE ACCESS AND FREE ALLOCATION OF POWER

In the communication scenario, we need to focus the signal on multiple targets and follow the target movement. At the same time, we need to adjust the correction coefficient of the transmitted signal according to the predicted received signal strength of each user to make a reasonable allocation of power.

In the above section, we built a light field model of a phased cell array and superimposed a Fourier field on it to eliminate the optical distortion caused by the lens group. In this section, we focus on the phase distribution of the phased cells and superimpose the independent Fourier light field on each optical phased cell to achieve the desired distribution of the light field and the free distribution of optical power.

First, we establish a desired light field distribution function according to the location of different users and the expected

received signal $r^{(k)'}(t)$ in Section 2.

$$V_0(x, y) = G(x, y)e^{i\theta(x,y)} \tag{17}$$

$G(x, y)$ represents the amplitude information of each phased cell, which is proportional to the amplitude of the expected received signal. Assuming that the light field transfer function is a pure phase function, since the approximate power loss in free space is zero, the desired light field function is

$$V(x, y) = e^{iG(x,y)\theta(x,y)} \tag{18}$$

Then, we encode the function into the form of the Fourier series

$$V(x, y) = \sum_{n=-\infty}^{\infty} V_n(x, y)e^{in\theta(x,y)} \tag{19}$$

In (19), the coefficient $V_n(x, y)$ is

$$V_n(x, y) = e^{i[n-G(x,y)]\pi} \frac{sin\{\pi [n - G(x, y)]\}}{\pi [n - G(x, y)]} \tag{20}$$

The n-level extension in (20) can be interpreted as forming different diffraction orders. Therefore, the function not only encodes the phase distribution $e^{in\theta(x,y)}$ but also encodes the amplitude information $G(x, y)$ in the coefficient $V_n(x, y)$. Among them, n = 0 and n = 1 are the two major components. The first diffraction order (n = 1) reproduces the original phase function $V(x, y)$ and performs amplitude modulation according to $V_n(x, y)$. When $G(x, y)$ increases from 0 to 1, $V_1(x, y)$ increases from 0 to 1 accordingly. Therefore, $V_1(x, y)$ roughly reproduces the original amplitude function $G(x, y)$, which is desired. We can use the first diffraction order to reproduce any desired composite transfer function according to (17). However, due to the *sinc* function in $V_n(x, y)$, the amplitude function $G(x, y)$ will be somewhat distorted. To solve this, we multiply $V_1(x, y)$ by the complex conjugate of the exponent factor, that is, retain the *sinc* function part,

$$V_1'(x, y) = \frac{sin\{\pi [1 - G(x, y)]\}}{\pi [1 - G(x, y)]} \tag{21}$$

Then we compensate for the distortion produced by the *sinc* function, construct a distortion compensation lookup table, and build the distortion modulation function $G''(x, y)$ accordingly. Finally we can get an ideal distortion-free function $V_1''(x, y)$, ie

$$V_1''(x, y) = \frac{sin\left\{\pi \left[1 - G''(x, y)\right]\right\}}{\pi [1 - G''(x, y)]} \tag{22}$$

The zeroth diffraction order (n = 0) roughly reproduces the rest of the light field after removing the original function. In (20), when $G(x, y)$ increases from 0 to 1, $V_0(x, y)$ decreases from 1 to 0 accordingly. The intensity of the zero-order diffraction order is inversely proportional to the magnitude of the original amplitude function, so $V_0(x, y)$ can be regarded as the complement function of the original function light field.

Therefore, the light field function $V_1''(x, y)e^{i\theta(x,y)}$ is superimposed on each phase cell, and after recovery through the lens group, the desired light field can be reproduced. Fig. 4 is a flow chart of the system. Fig. 5 is result of the light field recovery algorithm tested using a spatial light modulator (SLM).

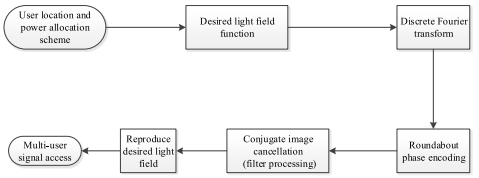

FIGURE 4. Flow chart of the optical space division multiple access system.

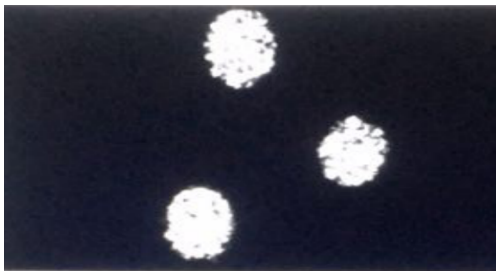

FIGURE 5. Desired light field reproduction.

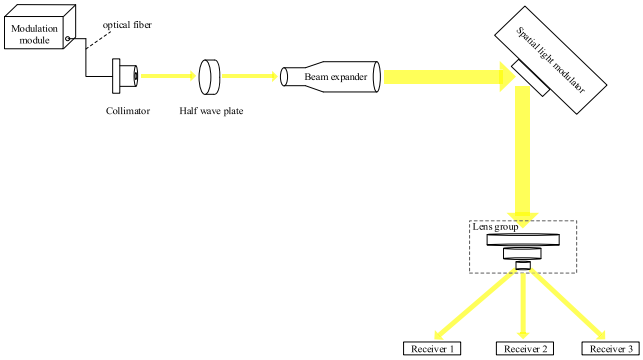

FIGURE 6. Experimental light path diagram.

V. EXPERIMENTAL SYSTEM CONSTRUCTION OF SMALL-SCALE OPTICAL ADAPTIVE ANTENNA ARRAY

This paper builds a small-scale optical adaptive antenna array to simulate SDMA and power allocation in real communication. We chose 532nm laser of 60mW as the light source (visible light is easy to observe), using a SLM to build a two-dimensional optical phased cell array, and a convex lens group for light field reproduction. Fig. 6 is an experimental light path diagram. The polarization of the half-wave plate used to rotate the laser causes the pixel elements in the SLM to only phase modulate it, and the amplitude does not change. The beam expander extends the laser beam to cover the SLM plane. The ultimate goal of the experiment is to focus the laser beam on multiple target points and to track the target and freely distribute power.

VI. EXPERIMENTAL RESULT

Power allocation. Fig. 7 is a photograph of the experimental system. We spatially divide the laser signal into three separate signals and measure whether their power distribution

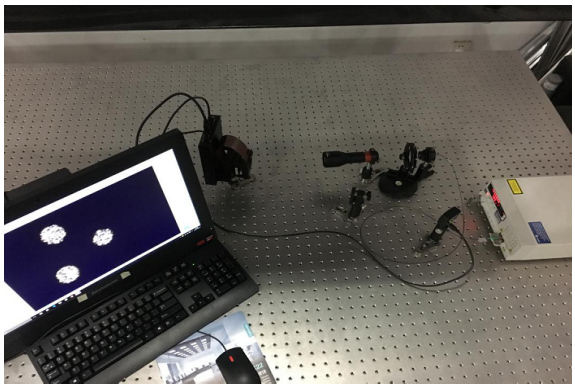

FIGURE 7. Experimental system for power allocation.

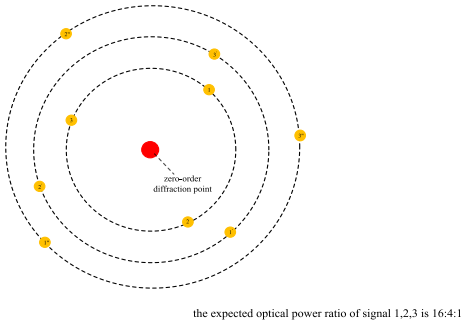

FIGURE 8. Schematic diagram of signals' position distribution.

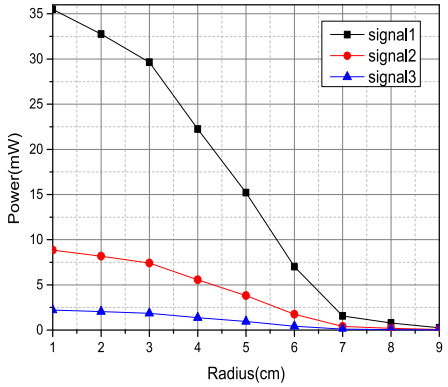

FIGURE 9. Power-radius curve.

matches the expected. In the experiment, we set the desired light field function to the sum of the three signals with an amplitude ratio of 4:2:1, so the expected optical power ratio is 16:4:1. However, according to [22]–[24], the distance from the zero-order diffraction point affects the diffraction efficiency of SLM, the closer the distance, the higher the diffraction efficiency. Therefore, in power distribution, the diffraction efficiency should be included in the adjustment of the correction factor. We then adjusted the three signals to the same distance as the zero-order diffraction point and measured their power.

Fig. 8 is a schematic diagram of the two-dimensional position distribution of three signals. The expected optical power ratio of signals 1, 2, 3 is 16:4:1. When constructing the desired light field function, they are all placed on the same circle

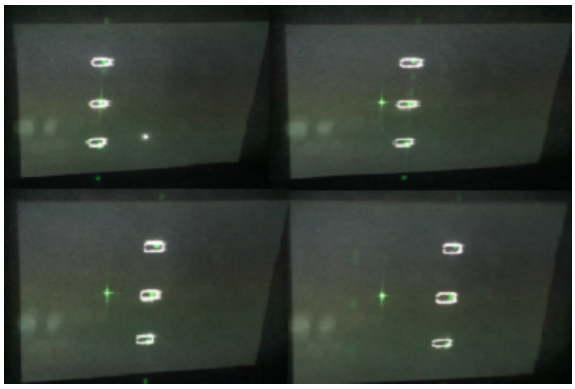

FIGURE 10. Target tracking test.

TABLE 1. Handing delays.

Link	Time
Target capture	0.08μs
Fourier superposition light field coding	0.134s
Control signal loading	9μs
SLM response	18ms

centered on the zero-order diffraction point. By measuring the power of the signals 1, 2, and 3 after the light field is reproduced and adjusting the radius of the circle, we can obtain multiple sets of measurement data. As shown in Fig. 9, on the circles of different radius, the power ratios of the signals 1, 2, and 3 are substantially maintained at 16:4:1, which is consistent with the desired optical power ratio. As the radius increases, the sum of the signal power decreases, and the diffraction efficiency decreases. Therefore, when setting the desired light field, it is necessary to consider the influence of the diffraction efficiency.

Target Tracking. Fig. 10 is a video capture of the three signals we have encoded following the movement of three targets. The still spot in the picture is a zero-order diffraction point. We use the ant colony algorithm and the simulated annealing algorithm for the locking and prediction of the target position, and initially realize the signal tracking of the low-speed fixed trajectory target.

Handling delays. Table 1 is the processing delay of each part of the system. In the future, it is desirable to integrate the positioning algorithm and the optical field recovery algorithm to further reduce the delay and improve the communication performance.

VII. CONCLUSION

This paper discusses an optically adaptive antenna array for SDMA and free power allocation in a multi-user OMC scenario. Compared with available alternatives, it takes into account the downlink point-to-multipoint communication under the optical mobile channel, that expands the application field of the optical phased antenna. Correspondingly, the technical idea of beamforming and space division multiplexing in 5G is extended to the optical frequency band.

Future research will refine and adjust the antenna array structure to improve energy efficiency and expand communication coverage. At the same time, the optical field recovery algorithm needs to be optimized to reduce the computational complexity and improve the performance of mobile communication under space division multiplexing.

REFERENCES

[1] S. D. Ilcev, "Space division multiple access (SDMA) applicable for mobile satellite communications," in *Proc. 10th Int. Conf. Telecommun. Mod. Satell. Cable Broadcast. Services (TELSIKS)*, Niš, Serbia, Oct. 2011, pp. 693–696.

[2] M. Hefnawi and A. Abubaker, "Channel capacity maximization in MIMO-SDMA based cognitive networks," in *Proc. Int. Conf. Multimedia Comput. Syst. (ICMCS)*, Marrakech, Morocco, Apr. 2014, pp. 1453–1456.

[3] O. González, M. F. Guerra-Medina, I. R. Martín, F. Delgado, and R. Pérez-Jiménez, "Adaptive WHTS-assisted SDMA-OFDM scheme for fair resource allocation in multi-user visible light communications," *J. Opt. Commun. Netw.*, vol. 8, no. 6, pp. 427–440, Jun. 2016.

[4] X. Liu, S. Xiao, and L. Quan, "Optical SDMA for applying compressive sensing in WSN," *J. Syst. Eng. Electron.*, vol. 27, no. 4, pp. 780–789, Aug. 2016.

[5] Z. Zhang, J. Dang, L. Wu, H. Wang, J. Xia, W. Lei, J. Wang, and X. You, "Optical mobile communications: Principles, implementation, and performance analysis," *IEEE Trans. Veh. Technol.*, vol. 68, no. 1, pp. 471–482, Jan. 2019.

[6] Z. Zhang, L. Wu, J. Dang, G. Zhu, J. Hu, H. Jiang, and X. You, "Optical mobile communications: Principles and challenges," in *Proc. 26th Wireless Opt. Commun. Conf. (WOCC)*, Newark, NJ, USA, Apr. 2017, pp. 1–4.

[7] N. Garcia, H. Wymeersch, E. G. Larsson, A. M. Haimovich, and M. Coulon, "Direct localization for massive MIMO," *IEEE Trans. Signal Process.*, vol. 65, no. 10, pp. 2475–2487, May 2017.

[8] Y. Mehmood, W. Afzal, F. Ahmad, U. Younas, I. Rashid, and I. Mehmood, "Large scaled multi-user MIMO system so called massive MIMO systems for future wireless communication networks," in *Proc. 19th Int. Conf. Autom. Comput.*, London, U.K., Sep. 2013, pp. 1–4.

[9] I. F. da Costa, S. A. Cerqueira, and D. H. Spadoti, "Dual-band slotted waveguide antenna array for adaptive mm-wave 5G networks," in *Proc. 11th Eur. Conf. Antennas Propag. (EUCAP)*, Paris, France, Mar. 2017, pp. 1322–1325.

[10] P. A. Dzagbletey and Y.-B. Jung, "Stacked microstrip linear array for millimeter-wave 5G baseband communication," *IEEE Antennas Wireless Propag. Lett.*, vol. 17, no. 5, pp. 780–783, May 2018.

[11] M. Rezk, W. Kim, Z. Yun, and M. F. Iskander, "Performance comparison of a novel hybrid smart antenna system versus the fully adaptive and switched beam antenna arrays," *IEEE Antennas Wireless Propag. Lett.*, vol. 4, pp. 285–288, 2005.

[12] L. Wu, Z. Zhang, J. Dang, and H. Liu, "Capacity lower bounds of IM/DD AWGN optical wireless channels based on Fano's inequality," in *Proc. Int. Conf. Wireless Commun. Signal Process. (WCSP)*, Nanjing, China, Oct. 2015, pp. 1–5.

[13] A. Al-Kinani, C.-X. Wang, L. Zhou, and W. Zhang, "Optical wireless communication channel measurements and models," *IEEE Commun. Surveys Tuts.*, vol. 20, no. 3, pp. 1939–1962, 3rd Quart. 2018.

[14] A. Raza and S. Muhammad, "Achievable capacity region of a Gaussian optical wireless relay channel," *J. Opt. Commun. Netw.*, vol. 7, no. 2, pp. 83–95, Feb. 2015.

[15] C. Gong and Z. Xu, "Channel estimation and signal detection for optical wireless scattering communication with inter-symbol interference,"*IEEE Trans. Wireless Commun.*, vol. 14, no. 10, pp. 5326–5337, Oct. 2015.

[16] J. He, "Optical system architecture design of multiple apertures array antenna for satellite-to-ground optical communication," in *Proc. Int. Conf. Space Opt. Syst. Appl. (ICSOS)*, Santa Monica, CA, USA, May 2011, pp. 343–345.

[17] Z. Li, W. Chuanhua, and L. Baoming, "Optical adaptive antenna array for free-space laser inter-satellites communication," in *Proc. Int. Conf. Comput. Sci. Inf. Technol.*, Singapore, Aug. 2008, pp. 907–910.

[18] Q. Tan, J. Wei, Z. Zhu, L. Dong, and X. Wang, "A novel cascaded optical phased array antenna with a phased wedge," in *Proc. 3rd Asia–Pacific Conf. Antennas Propag.*, Harbin, China, Jul. 2014, pp. 483–486.

[19] J. Yan, Z. He, C. Han, Y. Gao, and J. Cao, "Design and implementation of optical true time delay in optically controlled phased array antennas," in *Proc. CIE Int. Conf. Radar*, Shanghai, China, Oct. 2006, pp. 1–3.

[20] A. Wahab, T. B. Heok, and S. S. Erdogan, "Digital reconstruction of Fourier optical signal using efficient 24-bit floating point multiply-add-subtract module," in *Proc. IEEE Region 9th Annu. Int. Conf. Frontiers Comput. Technol. (TENCON)*, vol. 2, Aug. 1994, pp. 1049–1053.

[21] Z. Saraç, H. G. Birkök, H. Taşkın, and E. Öztürk, "Evaluation of thermal lens fringes using Hilbert and Fourier transform methods," *IET Sci., Meas. Technol.*, vol. 5, no. 3, pp. 81–87, May 2011.

[22] I. Moreno, A. Márquez, C. Iemmi, J. Campos, and M. J. Yzuel, "Modulation diffraction efficiency of spatial light modulators," in *Proc. 10th Euro-Amer. Workshop Inf. Opt.*, Benicàssim, Spain, Jun. 2011, pp. 1–4.

[23] A. K. Gupta and N. K. Nishchal, "Phase characterization of a liquid crystal spatial light modulator," in *Proc. 3rd Int. Conf. Microw. Photon. (ICMAP)*, Dhanbad, India, Feb. 2018, pp. 1–2.

[24] Y. Suzuki, "Spatial light modulators for phase-only modulation," in *Pacific Rim Conf. Lasers Electro-Opt. (CLEO/Pacific Rim) Tech. Dig.*, Seoul, South Korea, vol. 4, Aug. 1999, pp. 1312–1313.

HAIBO WANG received the B.S. degree in information engineering from Southeast University, Nanjing, China, where he is currently pursuing the M.S. degree in information and communications engineering. Since 2017, he has been with the National Mobile Communications Research Laboratory, Southeast University. His current research interests include optical mobile communications, and multiple input and multiple output wireless communication systems.

ZAICHEN ZHANG received the B.S. and M.S. degrees in electrical and information engineering from Southeast University, Nanjing, in 1996 and 1999, respectively, and the Ph.D. degree in electrical and electronic engineering from The University of Hong Kong, in 2002. From 2002 to 2004, he was a Postdoctoral Fellow with the National Mobile Communications Research Laboratory, Southeast University, where he is currently a Professor. He has authored over 200 papers and has issued 30 patents. His current research interests include 6G mobile information systems, optical wireless communications, and quantum information technologies.

JIAN DANG (M'15) received the B.S. degree in information engineering and the Ph.D. degree in information and communications engineering from Southeast University, Nanjing, China, in 2007 and 2013, respectively. From 2010 to 2012, he was a Visiting Scholar with the Department of Electrical and Computer Engineering, University of Florida, USA. Since 2013, he has been with the National Mobile Communications Research Laboratory, Southeast University, where he is currently an Associate Professor. His research interests include signal processing in wireless communications and optical mobile communications.

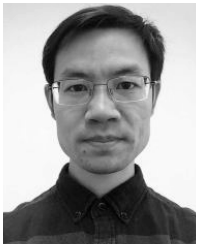

LIANG WU (M'13) received the B.S., M.S., and Ph.D. degrees from the School of Information Science and Engineering, Southeast University, Nanjing, China, in 2007, 2010, and 2013, respectively. From 2011 to 2013, he was a Visiting Student with the School of Electrical Engineering and Computer Science, Oregon State University. He is currently a Lecturer with the National Mobile Communications Research Laboratory, Southeast University. His research interests include indoor optical wireless communications, multiple input and multiple output wireless communication systems, and interference alignment.